International Journal of Progressive Sciences and Technologies (IJPSAT)
ISSN: 2509-0119.

https://ijpsat.org/
Vol. 47 No. 1 October 2024, pp. 387-393

Optimizing Wind Turbine Performance Using NACA 6409 Airfoil for Low to Moderate Wind Speeds: A Q-Blade Simulation Study

Hendry Sakke Tira[1], Arif Furqon[2]

[1]Mechanical Engineering department
University of Mataram
Mataram, Indonesia
hendrytira@unram.ac.id

[2]Mechanical Engineering department
University of Mataram
Mataram, Indonesia
ariffurqon1024@gmail.com

***Abstract*— This study aims to optimize the wind turbine design using the NACA 6409 airfoil through simulation based on the Q-Blade software. Wind turbines are a key technology in harnessing renewable energy, especially in areas with low to medium wind speeds. In this study, the NACA 6409 airfoil was selected due to its aerodynamic characteristics, which can generate high lift with low drag, thus increasing the efficiency of converting wind energy into mechanical energy. Simulations were carried out using the Blade Element Momentum (BEM) method to evaluate the turbine's performance at various angles of attack (AoA) and Tip Speed Ratios (TSR). The simulation results showed that the NACA 6409 airfoil could achieve a maximum power coefficient (Cp) at a TSR of 8, indicating optimal efficiency for the wind speed conditions modeled at the research location. Additionally, increasing the angle of attack resulted in an increase in lift coefficient (Cl) up to a critical point at 14°, where stall phenomena occurred, reducing aerodynamic performance. Pressure distribution around the airfoil was also analyzed to identify areas with the highest lift potential. This study concludes that a turbine design with the NACA 6409 airfoil can provide efficient performance in moderate wind speed conditions, making it a suitable solution for areas like Semayan Village, Lombok Island, Indonesia. The use of Q-Blade has proven effective in optimizing design and predicting turbine performance before a physical prototype is developed.**

***Keywords*— NACA 6409, Q-Blade, Blade Element Momentum, Semayan Village.**

I. INTRODUCTION

As global energy needs increase and fossil fuel reserves deplete, the world faces a significant challenge in seeking sustainable energy sources. Renewable energy, particularly wind energy, has emerged as a promising solution to reduce dependence on conventional energy sources, which have detrimental environmental impacts. According to various studies, wind energy has significant potential to meet the world's energy needs without leaving a substantial carbon footprint [1]. Additionally, wind is an abundant and widely distributed energy source, particularly in coastal areas and highlands with consistent wind intensity [2]. Therefore, the development of efficient wind turbine technology is becoming increasingly important to maximize this energy potential and meet the growing energy demand.

International Journal of Progressive Sciences and Technologies (IJPSAT)
ISSN: 2509-0119.

https://ijpsat.org/
Vol. 47 No. 1 October 2024, pp. 387-393

Wind turbines have become one of the key technologies in wind energy utilization. The efficiency of wind turbines is greatly influenced by the blade design, where the aerodynamic shape and profile determine how effectively wind energy can be converted into mechanical and electrical energy [3, 4]. One of the blade profiles commonly used in wind turbine design is the NACA (National Advisory Committee for Aeronautics) airfoil type. This profile is known for its ability to generate high lift while minimizing drag. Previous studies have shown that selecting the right airfoil profile, such as the NACA 6409, can significantly improve wind turbine performance [5]. An efficient blade design must be able to maximize the power coefficient at varying wind speeds and an optimal Tip Speed Ratio [6]. In this regard, simulation software such as Q-Blade is a highly useful tool in designing and testing wind turbine performance before a prototype is built. With the ability to analyze lift, drag, and airflow distribution around the blades, Q-Blade allows researchers to conduct more accurate and efficient design optimizations, enabling wind turbines to operate at maximum efficiency under specific wind conditions.

Q-Blade is software widely used in the design and performance simulation of wind turbines based on the Blade Element Momentum method. This software allows for detailed calculations of pressure distribution and aerodynamic forces on turbine blades, making it highly beneficial for evaluating optimal designs. Previous research has shown that simulations using Q-Blade can provide accurate predictions of wind turbine performance, particularly in terms of the power coefficient and the Tip Speed Ratio [7]. Additionally, Q-Blade supports various types of airfoil profiles, including the NACA 6409 used in this study, enabling analysis of different blade design variations. In prior studies, simulations using Q-Blade resulted in efficiency predictions for turbines that closely matched physical test results [8, 9]. Thus, using this software is considered very effective in designing wind turbines, especially for regions with specific wind characteristics such as Semayan Village, Lombok Island, Indonesia. In the context of this research, Q-Blade was used to model turbine performance based on local wind speed data, with the aim of optimizing the turbine design suitable for the local geographical and environmental conditions.

The NACA 6409 airfoil profile was selected in this study because of its superior aerodynamic characteristics for low to medium-speed wind turbines. This airfoil is known for its ability to generate high lift with relatively low drag, making it efficient in maximizing the conversion of wind energy into mechanical energy [10, 11]. Several previous studies have shown that the NACA 6409 airfoil can improve wind turbine performance in moderate wind speed conditions, making it ideal for areas like Semayan Village, where the average wind speed is not very high but remains stable throughout the year [12].

In this study, aerodynamic simulations of the wind turbine were conducted using the Q-Blade software, which is based on the Blade Element Momentum method. Q-Blade enables more detailed analysis of rotor performance, including calculating the power coefficient relative to the tip speed ratio. Previous studies have proven the reliability of Q-Blade in accurately modeling wind turbine performance, particularly in testing blade design variations and optimizing twist angles [13, 14]. By inputting wind speed data and the NACA 6409 airfoil parameters, this simulation is expected to provide a clear picture of the energy efficiency that can be achieved by the wind turbine at the study location.

II. Experimental Design

General Simulation Setting. The simulation steps were set with a timestep size of 0.00085404 seconds, which determines the time interval per simulation step. Each azimuthal step was carried out with an angle of 4.5°, and the total simulation was run in 6000 steps, resulting in an overall simulation duration of 5.105 seconds. These settings ensure that the simulation runs in sufficient detail to generate accurate data regarding the performance of the tested wind turbine.

Turbine Setup. The simulation was performed with the global position settings (X, Y, Z) set to (0, 0, 0), meaning the turbine was positioned at the center of the coordinate axis. The global rotation was also set to (0, 0, 0) degrees, indicating that there was no additional rotation on the main turbine axis. This setup ensures that the turbine simulation was performed in a standard position and orientation without the influence of additional rotations or displacements, facilitating the analysis of the specific performance of the turbine blades.

In the Rotational Speed Settings, the revolutions per minute value was set to 881.474, indicating the turbine blade rotation speed during the simulation. Additionally, the Tip Speed Ratio (TSR) was set to 8, which is the ratio between the tip speed of the turbine

International Journal of Progressive Sciences and Technologies (IJPSAT)
ISSN: 2509-0119.

https://ijpsat.org/
Vol. 47 No. 1 October 2024, pp. 387-393

blade and the wind speed. There are two options for TSR: Ramp-Up Fixed and Always Fixed. With this setting, the TSR was maintained at 8 throughout the simulation, meaning that the blades rotate at a speed proportional to the wind speed, making it easier to evaluate the turbine's power output performance under specific wind speed conditions. Proper TSR settings are crucial in optimizing the wind turbine's energy capture efficiency.

In Turbine Initial Conditions, the initial parameters for the turbine simulation include the yaw, pitch, and roll positions of the turbine. Each of these parameters was set to 0°, indicating that the simulation started without any tilt or additional rotation from the turbine's initial position. Yaw refers to the horizontal rotation of the turbine relative to the wind direction. Pitch indicates the blade tilt angle relative to the horizontal axis, and Roll is the turbine blade's rotation around its longitudinal axis. These zero initial values suggest that the turbine was positioned upright and aligned with the wind direction, providing an ideal basis for measuring turbine performance under normal conditions without the influence of other factors.

Structural Simulation Settings. The structural simulation settings include several key parameters. Structural Steps/AeroStep function to set the number of steps in the aerodynamic structure simulation, while Initial Relaxation Steps allow time for the simulation to stabilize and reduce numerical effects in the early steps. The parameter Number of Iterations was set to 100 iterations, meaning the simulation will run for 100 calculation cycles to obtain more accurate results. The option to include hydrodynamic forces and wind moments on the blade structure was also available. These settings help determine the effects of wind and aerodynamic pressure on the overall stability and efficiency of the turbine.

The geometry of the NACA 6409 airfoil is shown in Fig. 1. This airfoil is displayed in a 2D profile showing the thickness and camber distribution from the leading edge to the trailing edge. The following data provides detailed airfoil parameters as follows:

1. Foil Name: The airfoil used is NACA 6409, which represents an aerodynamic profile with a thickness of 9% of the chord (airfoil length).

2. Thickness: The maximum airfoil thickness is 9%, located at 29.50% of the airfoil chord. This means that the point of maximum thickness is near the front of the profile.

3. Camber: Camber refers to the curvature of the airfoil profile, indicating how curved the upper and lower surfaces are. The maximum camber of 6% is located at 40% of the chord, indicating optimal lift distribution for the simulated flight or speed conditions.

4. Points: There are 201 data points used to form the curve of this airfoil, providing sufficient resolution for aerodynamic analysis.

5. Leading Edge Flap (LE Flap): The LE flap angle is 0.00°, meaning no flap modification has been made on the leading edge for additional airflow control.

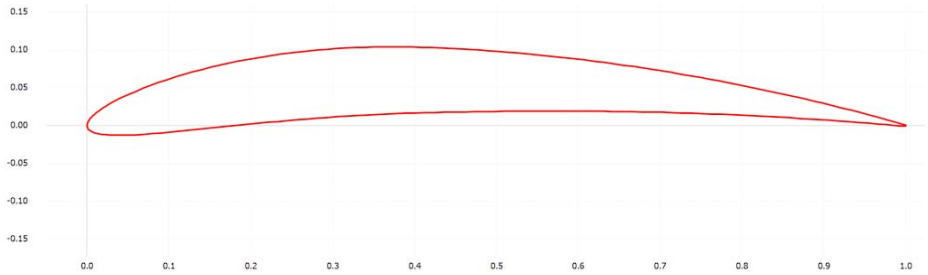

Fig. 1. Geometry design of airfoil NACA 6409

III. Results and Discussion

Fig. 2 shows the relationship between the lift coefficient and the angle of attack, demonstrating that the Cl value increases significantly as the angle of attack increases, reaching a maximum at around 14 degrees. After reaching this peak, the Cl value decreases, indicating stall. Stall occurs when the airflow around the airfoil begins to separate from its surface, causing a sudden loss

International Journal of Progressive Sciences and Technologies (IJPSAT)
ISSN: 2509-0119.

https://ijpsat.org/
Vol. 47 No. 1 October 2024, pp. 387-393

of lift [15]. At this point, even as the angle of attack continues to increase, the airfoil can no longer generate optimal lift because the airflow over the upper surface has separated.

This phenomenon aligns with basic aerodynamic theory, which states that increasing the angle of attack will increase lift by reducing the pressure on the upper surface of the airfoil while increasing pressure on the lower surface, creating a greater pressure differential. However, at a certain critical angle, typically between 10-15° depending on the airfoil design, airflow separation begins to occur, reducing the airfoil's ability to generate further lift. This result is consistent with literature stating that at the critical angle of attack, maximum lift is achieved, but after that, stall occurs, and aerodynamic performance declines [16].

The significant increase in lift coefficient at lower angles of attack also indicates that the airfoil has good aerodynamic efficiency in the low to medium angle of attack range, which is often utilized in aviation applications to maintain fuel efficiency and aircraft stability.

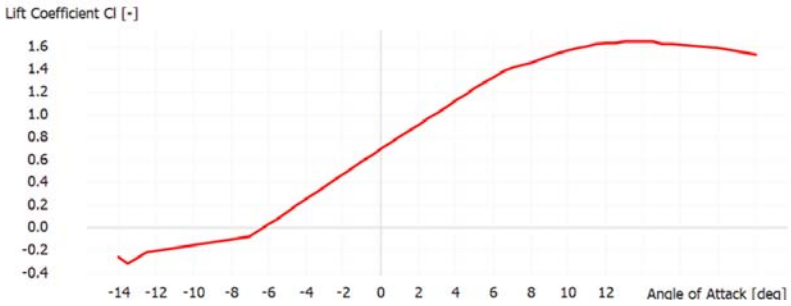

Fig. 2. Correlation beween coefficient of lift (Cl) and Angle of Attack (AoA)

Fig. 3 illustrates the pressure distribution around the airfoil under certain conditions. This pressure distribution is closely related to the amount of lift generated. On the upper surface of the airfoil, there is a larger negative pressure area (shown by red arrows), which contributes to generating lift. Meanwhile, on the lower side, higher pressure (with blue arrows) pushes the airfoil upward. This flow corresponds to Bernoulli's principle, where the difference in airflow speed between the upper and lower surfaces of the airfoil results in a pressure differential that produces lift.

Figs. 2 and 3 are related, as an increase in the angle of attack leads to a greater pressure differential between the upper and lower surfaces of the airfoil, resulting in an increase in lift, as shown in the Cl graph in Fig. 1. However, at higher angles of attack, the airflow over the airfoil becomes unstable, leading to the stall phenomenon, which reduces the lift coefficient, as previously discussed in prior studies [17].

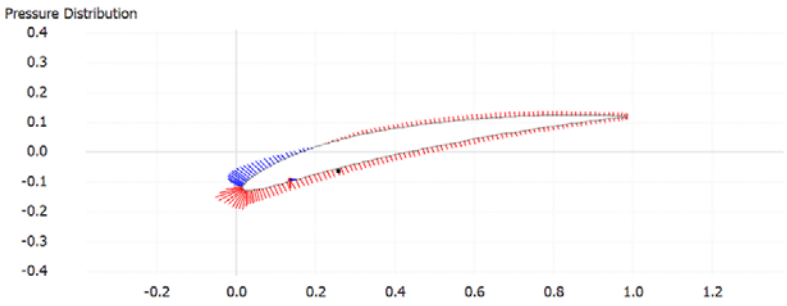

Fig. 3. Pressure Distribution around the Airfoil

Fig. 4 shows the relationship between the drag coefficient (Cd) and the angle of attack. This figure provides information on the amount of drag generated by the airfoil at various angles of attack.

At negative angles of attack up to about -14°, the drag coefficient is quite high, indicating that at these angles, the airflow around the airfoil is not optimal, leading to increased drag. As the angle of attack increases toward positive values, the drag

International Journal of Progressive Sciences and Technologies (IJPSAT)
ISSN: 2509-0119.

https://ijpsat.org/
Vol. 47 No. 1 October 2024, pp. 387-393

coefficient drastically decreases, reaching its minimum at around 0°. At this point, the drag generated by the airfoil is at its lowest, indicating optimal aerodynamic conditions where the airflow around the airfoil is relatively stable and not experiencing separation.

However, as the angle of attack increases beyond approximately 4-6°, the drag coefficient starts to rise again. This is due to the increasing angle of attack, which disturbs the airflow around the airfoil. The increase in drag at higher angles of attack is often associated with flow separation, where the airflow over the upper surface of the airfoil detaches from the airfoil surface, reducing aerodynamic efficiency and increasing drag.

Overall, this figure shows that at low angles of attack (near 0°), the drag generated is very small, but at excessively high or low angles of attack (both negative and positive), drag increases significantly. This decrease in efficiency is related to aerodynamic effects that cause the airflow around the airfoil to become turbulent or separate from the airfoil surface.

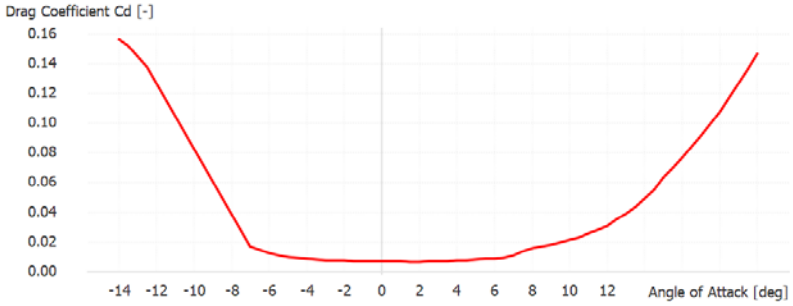

Fig. 4. Correlation between Drag Coefficient (Cd) and Angle of Attack

Fig. 5 presents the relationship between sound pressure level (SPL) and frequency, showing that the SPL peaks at low frequencies (around 10^2 Hz) with values reaching up to 90 dB, then significantly decreases at medium to high frequencies, especially approaching 10^4 Hz, where the SPL approaches 0 dB. This SPL reduction is due to several key factors.

First, air absorption is more effective at high frequencies, where air molecules absorb more sound energy, causing sound waves to attenuate more quickly. Second, sound propagation patterns at low frequencies are more evenly distributed and not easily absorbed, whereas at high frequencies, sound is more directional and experiences more reflections, which accelerate the reduction of SPL. Third, peaks at certain mid-range frequencies are likely caused by resonance, where sound is amplified before the SPL drops sharply.

These results are consistent with previous studies showing that high frequencies dissipate more quickly, while low frequencies persist longer in their propagation [18]. This is important in acoustic design, particularly for sound dampening solutions that need to effectively handle high-frequency spectrums. The results confirm that low frequencies produce a more stable SPL compared to high frequencies, which require special attention in sound dampening applications.

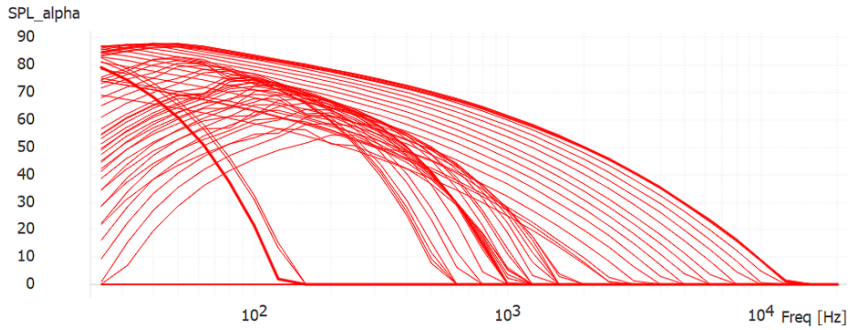

Fig. 5. Sound Pressure Level (SPL) vs Frequency

IV. Conclusion

This study successfully identified the optimal performance of a wind turbine using the NACA 6409 airfoil through software-based simulations using Q-Blade. The simulation results demonstrated that the NACA 6409 airfoil possesses aerodynamic characteristics suitable for wind turbine applications in areas with low to moderate wind speeds, such as Semayan Village. The turbine's maximum efficiency was achieved at a Tip Speed Ratio (TSR) of 8, with an optimal power coefficient (Cp), indicating efficient wind energy conversion.

Additionally, the pressure distribution study around the airfoil showed that the optimal angle of attack before stall occurred was 14°, which plays a crucial role in maximizing lift and reducing drag. Therefore, the NACA 6409 airfoil offers an effective solution to improve wind turbine performance under varying wind conditions.

The simulation using Q-Blade has proven to provide accurate predictions of turbine performance, minimizing risks in the design process before physical prototype development. The conclusions of this study affirm that wind turbine designs utilizing the NACA 6409 airfoil can be efficiently implemented in moderate wind environments and have the potential to enhance the application of renewable energy in such areas.

References

[1] G. Msigwa, J.O. Ighalo, and P.S. Yap, "Considerations on environmental, economic, and energy impacts of wind energy generation: Projections towards sustainability initiatives," Science of The Total Environment, vol. 849, p. 157755, Nov. 2022.

[2] J. Li, G. Wang, Z. Li, S. Yang, W.T. Chong, and X. Xiang, "A review on development of offshore wind energy conversion system," International Journal of Energy Research, vol. 44, no. 12, pp. 9283-9297, Oct. 2020.

[3] J. Beauson, A. Laurent, D.P. Rudolph, and J.P. Jensen, "The complex end-of-life of wind turbine blades: A review of the European context," Renewable and Sustainable Energy Reviews, vol. 155, p. 111847, Mar. 2022.

[4] D.A. Katsaprakakis, N. Papadakis, and I. Ntintakis, "A comprehensive analysis of wind turbine blade damage," Energies, vol. 14, no. 18, p. 5974, Sep. 2021.

[5] A. Tokul, and U. Kurt, "Comparative performance analysis of NACA 2414 and NACA 6409 airfoils for horizontal axis small wind turbine," International Journal of Energy Studies, vol. 8, no. 4, pp. 879-898, 2023.

[6] V. Durgesh, H. Johari, and E. Garcia, "Aerodynamic behavior and flow visualization on canonical NACA airfoils at low Reynolds number," Journal of Visualization, vol. 26, no. 4, pp. 795-814, Aug. 2023.

[7] P. Koragappa, and P.G. Verdin, "Design and optimisation of a 20 MW offshore wind turbine blade," Ocean Engineering, vol. 305, p. 117975, Aug. 2024.

[8] A. Suresh, and S. Rajakumar, "Design of small horizontal axis wind turbine for low wind speed rural applications," Materials Today: Proceedings, vol. 23, pp. 16-22, Jan. 2020.

[9] M.A. Rahmanta, and A. Aprilana, "Designing of 500 watt wind turbine blades for manufacturing," in AIP Conference Proceedings, vol. 2403, no. 1, AIP Publishing, Dec. 2021.

[10] K. Chandan, S. Devi, and K.V. Nagaraja, "Effective evaluation of aerodynamic characteristics using subparametric finite element transformation for unmanned air vehicles at low Reynolds number," Materials Today: Proceedings, Sep. 2023.

[11] M. Thianwiboon, "A Numerical Comparative Study of the Selected Cambered and Reflexed Airfoils in Ground Effect," Engineering Journal, vol. 27, no. 11, pp. 39-51, Nov. 2023.

[12] Y. Wang, R. Zou, F. Liu, L. Zhang, and Q. Liu, "A review of wind speed and wind power forecasting with deep neural networks," Applied Energy, vol. 304, p. 117766, Dec. 2021.

[13] S. Ali, and C.M. Jang, "Effects of tip speed ratios on the blade forces of a small H-darrieus wind turbine," Energies, vol. 14, no. 13, p. 4025, Jul. 2021.

[14] J.I. Encarnacion, and C. Johnstone, "Levelised Cost of Energy for High Tip-Speed Ratio Tidal Turbines Operating in Less Energetic Flows," Chemical Engineering Transactions, vol. 103, pp. 247-252, Oct. 2023.

[15] S. Le Fouest, and K. Mulleners, "The dynamic stall dilemma for vertical-axis wind turbines," Renewable Energy, vol. 198, pp. 505-520, Oct. 2022.

[16] N.M. Tousi, M. Coma, J.M. Bergadà, J. Pons-Prats, F. Mellibovsky, and G. Bugeda, "Active flow control optimisation on SD7003 airfoil at pre and post-stall angles of attack using synthetic jets," Applied Mathematical Modelling, vol. 98, pp. 435-464, Oct. 2021.

[17] M. Masdari, M. Mousavi, and M. Tahani, "Dynamic stall of an airfoil with different mounting angle of gurney flap," Aircraft Engineering and Aerospace Technology, vol. 92, no. 7, pp. 1037-1048, Jun. 2020.

[18] J. Tougaard, L. Hermannsen, and P.T. Madsen, "How loud is the underwater noise from operating offshore wind turbines?," The Journal of the Acoustical Society of America, vol. 148, no. 5, pp. 2885-2893, Nov. 2020